Effective Method for Dispersing SiO_2 Nanoparticles into Polyethylene

Maija Pöllänen, Uwe Pelz, Mika Suvanto, Tuula T. Pakkanen

Department of Chemistry, University of Joensuu, Joensuu 80101, Finland

Received 17 June 2008; accepted 26 October 2009
DOI 10.1002/app.31673
Published online 17 December 2009 in Wiley InterScience (www.interscience.wiley.com).

ABSTRACT: An effective solution mixing method starting from a synthesis solution of SiO_2 nanoparticles was developed for dispersing nanoparticles into high-density polyethylene (HDPE). Spherical SiO_2 nanoparticles with narrow size distribution (50–100 nm) were prepared by Stöber method, and solvents of the synthesis solution (EtOH/NH_4OH) were gradually replaced with toluene by evaporation under reduced pressure. The SiO_2 nanodispersion, in toluene and residual ethanol, was mixed and refluxed with dissolved maleic anhydride grafted polyethylene (PE*g*MA) at a relatively high SiO_2 content (17.8 wt %). The PE*g*MA-SiO_2 masterbatch was filtered, dried under vacuum, and mixed with HDPE by melt compounding. SiO_2 contents in the final HDPE nanocomposites were 3 and 5 wt %. SEM images of the masterbatch and final composites showed the SiO_2 nanoparticles to be well dispersed in HDPE. No agglomerates were observed. FTIR results suggest that the interactions between the maleic anhydride group of PE*g*MA and hydroxyl groups of SiO_2 surface involve ester and/or hydrogen bonding. Addition of SiO_2 particles and PE*g*MA to HDPE slightly increased Young's modulus, tensile strength, breaking strength, and elongation at break, indicating enhanced toughness of the nanocomposites. The measured Young's moduli of HDPE-PE*g*MA-SiO_2 composites agreed well with Young's moduli predicted by Mori-Tanaka composite theory. © 2009 Wiley Periodicals, Inc. J Appl Polym Sci 116: 1218–1225, 2010

Key words: nanocomposites; polyethylene; nanodispersions; nanoparticles; SiO_2

INTRODUCTION

Polymer nanocomposites represent a new and rapidly developing area of materials research. Nanoparticles, which have at least one dimension less than 100 nm, are added as filler material to polymers to create nanocomposites with tailored physical and mechanical properties. The filler content may be very low, usually from 1 to 10 wt % suffices. Composites containing nanomaterials have several advantages over composites containing micron-sized filler, including the lighter weight of the final product and enhanced processing properties.[1,2]

The preparation of nanocomposites presents several challenges. Most important is the proper dispersion of nanoparticles into the polymer matrix; the small size of the nanoparticles leads to high surface energy, and the nanoparticles easily agglomerate. Achieving enhanced properties of nanocomposites also depends on a strong interaction between the nanoparticles and matrix. Most polymers are hydrophobic, and pretreatment of the nanoparticles, e.g., hydrophilic metal oxide nanoparticles, is often required to make particles and polymers chemically compatible.[3–5]

The synthesis of spherical SiO_2 particles in ethanol solution was published by Stöber et al.[6] in 1968. The method has subsequently been modified, and SiO_2 nanoparticles prepared by the Stöber method have been widely studied.[7–12] The Stöber method makes it possible to alter the size and morphology of the formed SiO_2 particles merely by changing the proportion of reagents.[6] The particle size can be varied from a few nanometers to a few micrometers.[7]

Only a few publications discuss polymer nanocomposites with Stöber-like nanoparticles as fillers.[8,9,11,12] In studies of the mechanical and tribological properties of epoxy nanocomposites, Zheng et al.[8] found that modified spherical SiO_2 nanoparticles (50 nm) decrease the friction coefficient and increase the fracture toughness and tensile strength of epoxy resin.[8] Ke et al.[9] encapsulated modified SiO_2 particles into polystyrene (PS) and incorporated the SiO_2-PS composite particles into polyethylene terephthalate matrix (PET). The PS-SiO_2 composite particles were well dispersed in PET and accelerated the crystallization by acting as nucleation centers.[9]

The main methods of preparing polyolefin-based nanocomposites are melt mixing,[13–15] *in situ* polymerization,[16,17] and solution mixing.[18] Of these

Correspondence to: T. T. Pakkanen (Tuula.Pakkanen@joensuu.fi).

Contract grant sponsors: Finnish Funding Agency for Technology and Innovation (Tekes) and European Union/European Regional Development Fund.

methods, the last two are carried out in solution phase, where high dispersions of nanoparticles can be achieved and maintained during the preparation by adjusting the surface chemistry of the nanoparticles. The preparation of polyethylene nanocomposites by solution mixing introduces the special problem that polyethylene dissolves in only a few common solvents and dissolution requires elevated temperatures.[13] Because it lacks reactive functional groups, polyethylene is also one of the most challenging polymer matrices for creating a chemical coupling with nanoparticles.

We set out to find a straightforward method based on solution-state mixing and, starting from the synthesis solution of SiO_2, to produce SiO_2 nanodispersions in high-density polyethylene (HDPE). PE*g*MA was used as a coupling agent to enhance the chemical compatibility between the polyethylene matrix and nanosized SiO_2 particles. FTIR was used to characterize the interactions. The nanosized SiO_2 particles were expected to influence the thermal and mechanical properties of HDPE, and these were studied by thermogravimetric analysis (TGA), differential scanning calorimetry (DSC), and tensile testing. The measured Young's moduli of HDPE-PE*g*MA-SiO_2 composites were compared with the Young's moduli of composites predicted by Mori-Tanaka composite theory.

EXPERIMENTAL

Materials

Ethanol (EtOH, Altia, 99.5%), tetraethoxysilane (TEOS, Acros Organics, 98%), ammonia solution (NH_4OH, J.T. Baker, 25% in water), toluene (Riedel-de Haën, 99.7%), and xylene (mixture of isomers and ethyl benzene, Sigma-Aldrich) were used as received. The HDPE (No. CG8410) was purchased from Borealis Polymers Oy. The melt flow rate of HDPE ($\rho = 0.941$ g/cm^3) was 7.5 g/10 min and the melting range was 110–140°C. Maleic anhydride grafted polyethylene (PE*g*MA, Polybond 3009) with maleic anhydride level of 1 wt % was from Crompton-Uniroyal Chemical. The melt flow rate of PE*g*MA ($\rho = 0.95$ g/cm^3) was 5.6 g/10 min and the melting point 127°C.

Synthesis of SiO_2 nanoparticles

Ethanol (1000 mL) and ammonia solution (60 mL) were mixed in a reaction flask. TEOS (50 mL) was added and the mixture was stirred overnight at room temperature. The formation of SiO_2 particles was observed as a white turbidity.

Preparation of SiO_2 nanocomposites

Part of the synthesis solution (EtOH/NH_4OH) of the SiO_2 nanoparticles was replaced with toluene using a rotary evaporator under reduced pressure (60°C water bath, 200–120 mbar). The synthesis solution (1000 mL) was placed in a 2000-mL round-bottomed flask, 400 mL of toluene was added, and the solution was partially evaporated to decrease the volume of ethanol. Three cycles of toluene addition (3 × 200 mL) and evaporation were carried out until a small amount of SiO_2 precipitate appeared and, in all, 870 mL of solvent was evaporated. The white precipitate was removed by filtration. The filtrate was a slightly turbid SiO_2-toluene-ethanol mixture. The pH of the mixture was about 7 indicating that all NH_4OH had been removed.

PE*g*MA (40.5 g) was added to a reaction flask with a ball condenser containing 400 mL of toluene, and the mixture was heated under magnetic stirring until the PE*g*MA dissolved in the toluene. Addition of the SiO_2-toluene-ethanol mixture (700 mL) to refluxing toluene solution of PE*g*MA caused a white precipitate to form. The precipitate was dissolved by switching off the water flow of the condenser and evaporating part of the solvent to remove ethanol. Then, 300 mL of toluene was added to compensate for the loss of solvent, and the mixture was stirred and heated until it was clear. The mixture was allowed to cool without stirring, and the PE*g*MA began to crystallize. The precipitate was filtered, washed with 700 mL of ethanol, and dried under vacuum. The product, the PE*g*MA-SiO_2 masterbatch, was a white powder.

The final composites were produced using this PE*g*MA-SiO_2 masterbatch as SiO_2 source and blending it with HDPE by melt compounding. Melt compounding of polyethylene composites was made with a DSM Midi 2000 extruder, and injection molding of test specimens was done with a DSM microinjection molding instrument. The melt compounding of composites was performed under a nitrogen atmosphere with a screw temperature of 200°C, a screw rotation speed of 100 rpm, and a dwell time of 5 min. Injection molding of the mechanical test specimens was done with a piston pressure of 4–6 bar, a temperature of feed unit of 180°C and a mold temperature of 40°C.

Characterization

SiO_2 nanoparticles were characterized by scanning electron microscopy (Hitachi S-4800). Samples, where SiO_2 particles were in solution, were prepared by the following method. A small amount of SiO_2 solution was diluted in ethanol, one drop of diluted

solution was placed on a copper grid with a lacey carbon film, and the sample was left to dry.

The masterbatch powder was anchored on the SEM sample stage with carbon tape, and the dispersion of the SiO_2 nanoparticles was characterized by SEM.

The final dispersion of SiO_2 nanoparticles in HDPE was observed from cut surfaces of the composites by SEM. Slides of the composites (40 μm) were cut with a Leica RM2165 rotary microtome with steel blade. Slides were coated with Pt/Pd alloy (layer thickness of 1.5–2 nm) to facilitate the measurements.

Composite samples for scanning transmission electron microscopy (STEM) measurements were prepared by dissolving a small amount of composite sample in boiling xylene, placing one drop of this solution on a copper grid and leaving the drop to dry.

FTIR spectra were measured with a Nicolet Magna 750 FTIR spectrometer with scanning range of 600–4000 cm^{-1}. FTIR spectra of SiO_2 and the PE*g*MA-SiO_2 masterbatch were measured using KBr tablets. The FTIR spectrum of PE*g*MA was recorded from a thin film of melted (190°C, 5 min) PE*g*MA.

TGA was made to determine the decomposition temperature of the samples and the amounts of SiO_2 in the masterbatch and in composites. TGA measurements were performed on a Mettler Toledo TGA/STDA851[e] under a nitrogen gas flow (50 mL/min) between 25 and 600°C with a heating rate of 20°C/min. Three measurements were made of each sample, and the average of the measurements was calculated. The decomposition temperature of the samples was determined as the intercept of the inflectional tangent with the baseline before the transition. The nanofiller content of the masterbatch and composites was determined by evaluating the mass loss of the polymer from the horizontal baselines of the TGA curves.

DSC was carried out on a Mettler Toledo DSC823[e]. Measurements were done under a nitrogen gas flow (50 mL/min) between 25 and 200°C with heating rate of 10°C/min. The DSC program included two heating–cooling cycles. In the first heating–cooling cycle, the thermal history of the sample was removed, and in the second cycle, the thermogram was recorded and the crystallinity of the sample determined. Three parallel measurements were made for each sample, and the crystallinity of

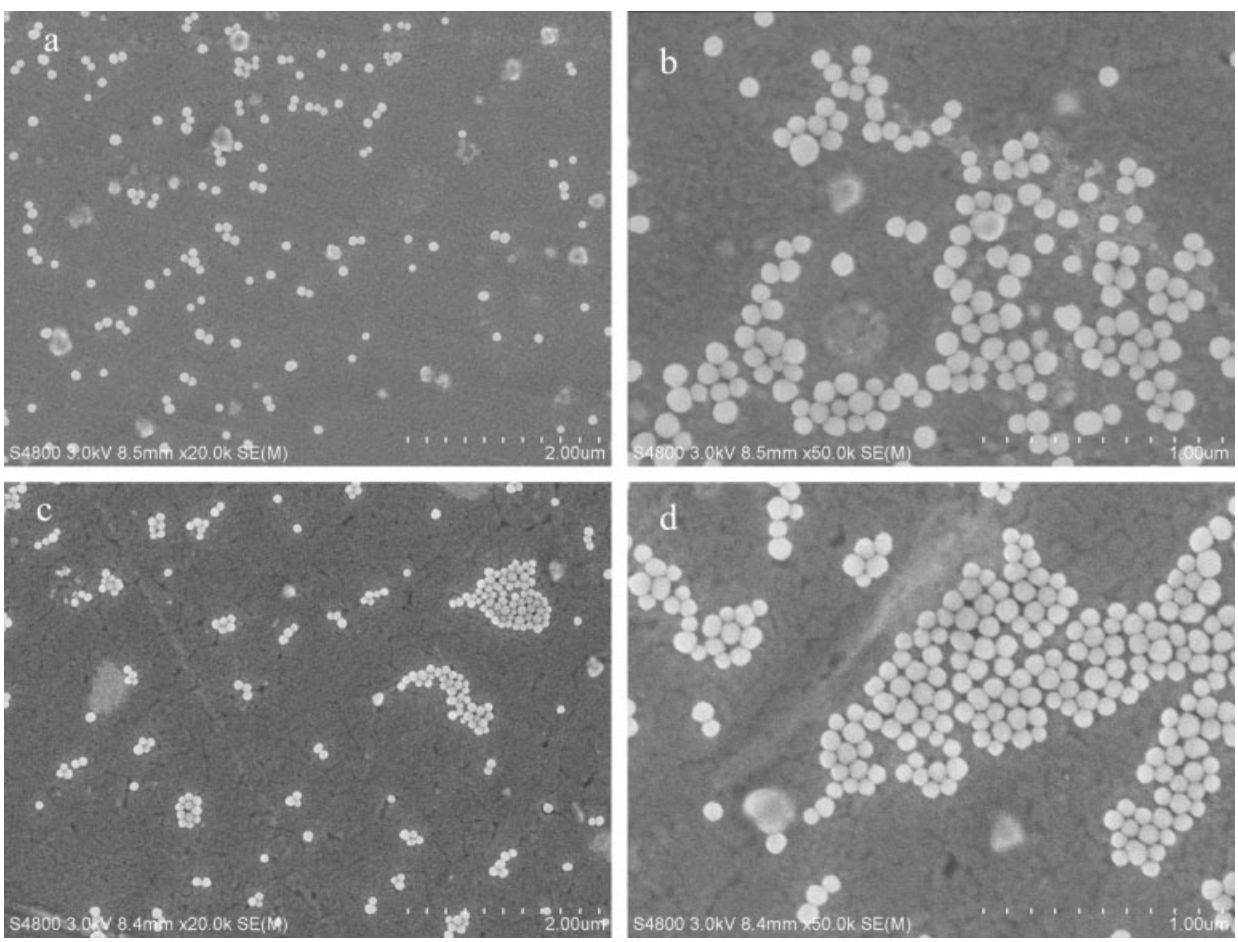

Figure 1 SEM images of SiO_2 nanoparticles in synthesis solution (a,b) and in toluene–ethanol mixture (c,d).

the sample is reported as the average of the three measurements. The integrated area between the melting profile and baseline was determined over a temperature range of 80–140°C, and the crystallinity was calculated assuming a linear relationship between the crystallinity and the integrated area corresponding to the melting enthalpy. For the samples containing SiO_2, the SiO_2 content obtained from TGA determination was subtracted from the sample mass. Crystallization temperatures of the samples were determined from the second heating–cooling cycle as the peak temperature of the crystallization (cooling) curve.

Mechanical testing of composites was carried out on material testing equipment (Zwick Z010/TH2A model 2001) with a crosshead speed of 50 mm/min. Calculations were performed with TestXpert version 8.1 software. Six standard tensile specimens were tested for each series.

The Young's modulus of composites containing micron-sized fillers can be predicted by a model based on Mori-Tanaka composite theory. The principles and details of the theory have been presented elsewhere.[19–22] According to Tandon and Weng,[21] the longitudinal and transverse modulus (E_{11} and E_{22}) of composites are expressed with the following equations.

$$\frac{E_{11}}{E_m} = \frac{\mathrm{A}}{\mathrm{A} + \Phi_f(\mathrm{A}_1 + 2\nu_m \mathrm{A}_2)} \quad (1)$$

$$\frac{E_{22}}{E_m} = \frac{2\mathrm{A}}{2\mathrm{A} + \Phi_f[-2\nu_m \mathrm{A}_3 + (1-\nu_m)\mathrm{A}_4 + (1+\nu_m)\mathrm{A}_5 \mathrm{A}]} \quad (2)$$

where E_m and ν_m are the Young's modulus and Poisson's ratio of the matrix and Φ_f is the volume fraction of the filler. Functions of Eshelby's tensor (A, A_1, A_2, A_3, A_4, and A_5) depend on properties of the filler and matrix. For spherical particles, the composite stiffness tensor is isotropic and $E_{11} = E_{22}$.[19–22]

Density of 2.204 g/cm^3, Poisson's ratio of 0.1763, and Young's modulus of 74.58 GPa for SiO_2 were used for the calculations.[23] Young's moduli measured for HDPE-PE*g*MA reference samples (0.67–0.65 GPa) were used as Young's moduli of the matrix. Poisson's ratio for HDPE (0.35) is according to the literature.[24,25]

RESULTS AND DISCUSSION

Synthesis of SiO_2 nanoparticles and preparation of SiO_2 nanocomposites

In the synthesis of the nanometer-sized SiO_2 particles from TEOS by Stöber method, part of the synthesis solution containing aqueous NH_3 and ethanol was replaced with toluene by evaporation under reduced pressure. The aim of this solvent exchange was to alter the solution environment of the SiO_2 particles: dispersion of SiO_2 nanoparticles into PE*g*MA by solution mixing is more favorable when the nanoparticles are present in toluene–ethanol mixture rather than in pure ethanol. Ethanol has a lower boiling point than toluene and could cause strong foaming during the solution mixing of SiO_2 and PE*g*MA. Solvent exchange in the SiO_2-ethanol solution used in Stöber synthesis proved feasible and has previously been applied[26] for surface modification of SiO_2 nanoparticles.

SiO_2 nanoparticles in toluene–ethanol mixture were mixed with maleic anhydride grafted polyethylene (PE*g*MA) dissolved in toluene to produce a PE*g*MA-SiO_2 masterbatch with high SiO_2 content (17.8 wt %, based on TGA). The masterbatch was filtered and dried under vacuum to remove the solvent residue. Melt compounding of the masterbatch with HDPE gave HDPE-PE*g*MA-SiO_2 nanocomposites with SiO_2 contents of 3 or 5 wt % according to TGA. PE*g*MA content in the composites was 14 and 23 wt %, respectively.

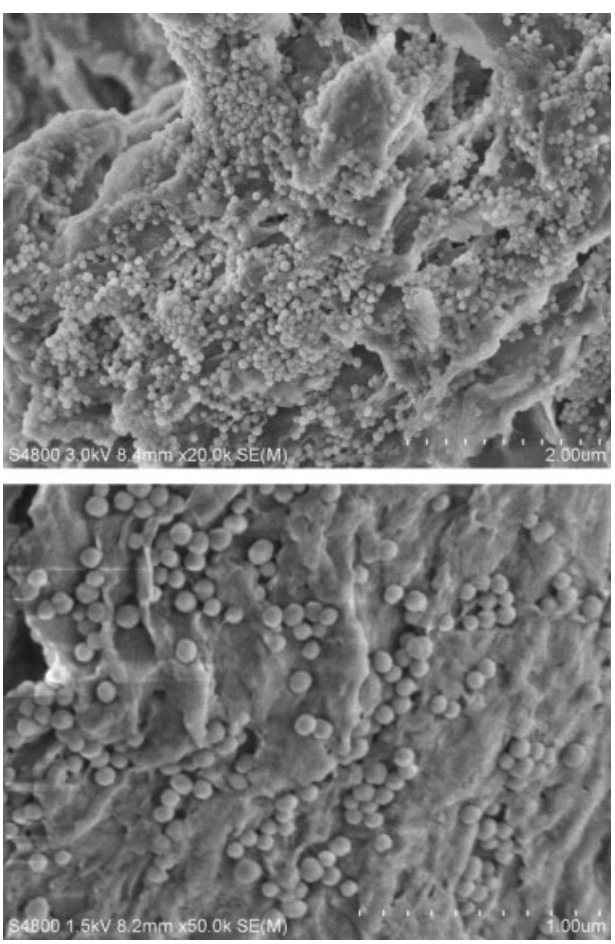

Figure 2 SEM images of PE*g*MA-SiO_2 masterbatch with SiO_2 content of 17.8 wt %.

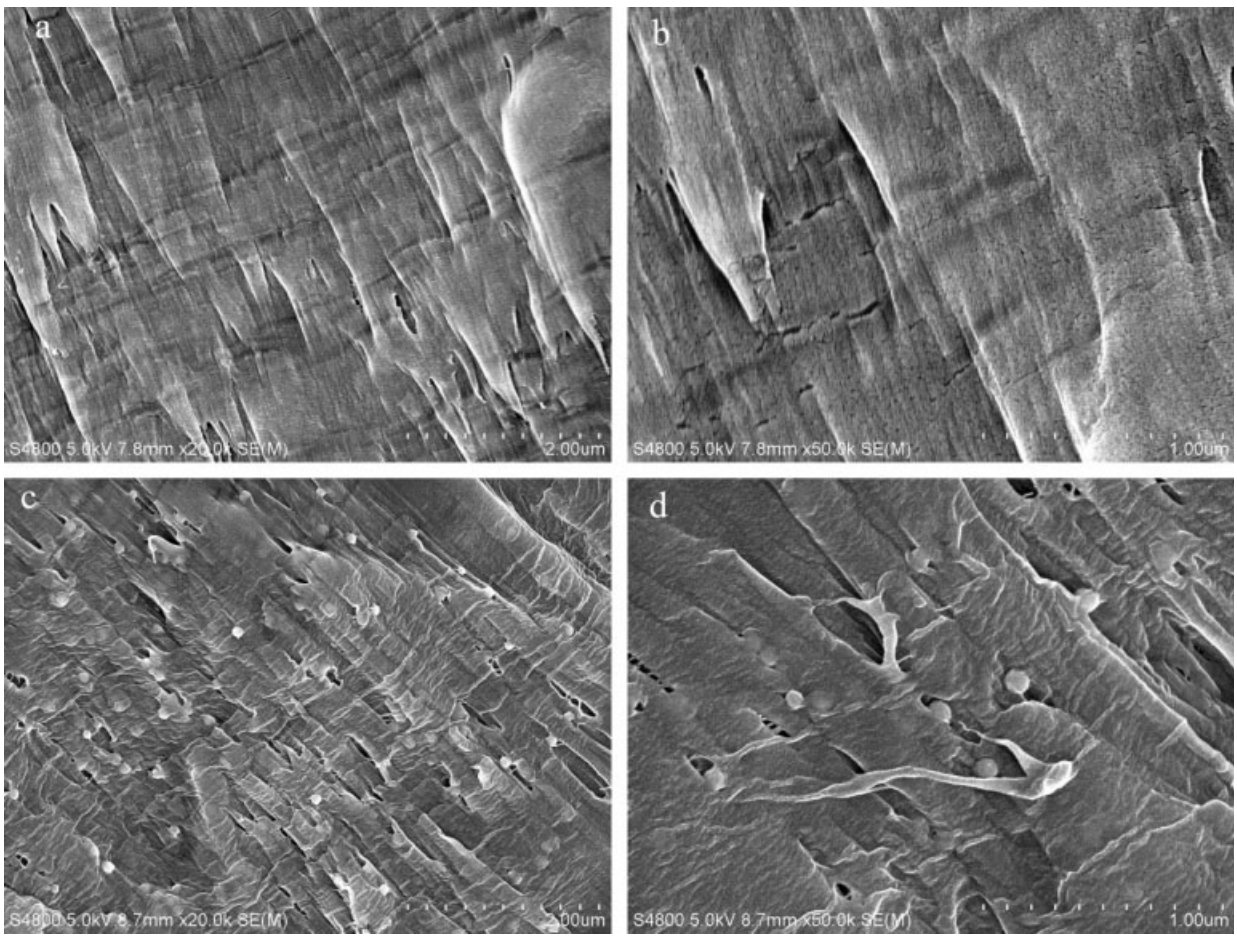

Figure 3 SEM images of cut surface of HDPE-PE*g*MA (30 wt %) reference (a,b) and HDPE-PE*g*MA (23 wt %)-SiO_2 (5 wt %) composite (c,d).

SEM characterization of SiO_2 dispersions at different stages of preparation

SiO_2 particles appeared in the synthesis solution ($EtOH/NH_4OH$) as a white turbidity. SEM observations showed the SiO_2 particles to have a narrow size distribution, 50–100 nm. Nanoparticles were well separated on the copper grid, indicating a high dispersion in the synthesis solution [Figure 1 (a,b)].

After addition of toluene and evaporation of part of the solution, the SiO_2-toluene-ethanol mixture was only slightly turbid, and occasionally, a blue color could be seen. We found that, in the replacement of the synthesis solution with toluene, some ethanol had to be left in the mixture to prevent agglomeration of the SiO_2 particles. Evidently, ethanol stabilizes the surface of the particles in nonpolar toluene. According to Ghosh et al.,[27] SiO_2 nanoparticles are stable in supercritical ethanol even at high pressures, and over a wide temperature range of 25–300°C. The exact proportions of solvents in the SiO_2-toluene-ethanol mixture were not determined; the evaporation was merely halted when a small precipitation of white solid was seen in the mixture. SEM images of SiO_2 nanoparticles in the SiO_2-toluene-ethanol mixture are presented in Figure 1 (c,d). Good separation of the particles on the copper grid indicates that the particles remain nanodispersed during the solvent exchange procedure.

Solution mixing is a promising method to disperse SiO_2 nanoparticles in PE*g*MA because it does not involve drying of particles, which may lead to agglomeration.[10,14] Figure 2 presents a high-level dispersion of SiO_2 nanoparticles in PE*g*MA. The amount of SiO_2 particles in the PE*g*MA-SiO_2 masterbatch is relatively high, which could cause some clustering of the particles. Although some of the particles could have been washed out during the preparation and washing of the masterbatch, most of them appear to stay in the PE*g*MA. This indicates interaction between the nanoparticles and PE*g*MA matrix. The retention of particles in PE*g*MA was confirmed by SEM analyses of the filtrate and ethanol washing solutions: only a few particles were found.

Dispersions of SiO_2 particles in the HDPE-PE*g*MA-SiO_2 composites were studied by SEM. The

cut surfaces of the HDPE-PE*g*MA (30 wt %) reference sample and HDPE-PE*g*MA (23 wt %)-SiO_2(5 wt %) composite are presented in Figure 3. The SEM image of the HDPE-PE*g*MA (30 wt %) reference shows good compatibility between HDPE and PE*g*MA. SiO_2 particles in HDPE-PE*g*MA were uniformly dispersed, and no agglomerations were present.

The degree of agglomeration in composites was also studied by STEM. Since STEM characterization requires a very thin sample (<100 nm), films were specially prepared for the purpose by placing a drop of the composite solution in hot xylene on a copper grid. Figure 4 shows that the SiO_2 particles are well separated. Since dissolving the composite in xylene would not be sufficient to break down any agglomerates, the results confirm the SEM observations, namely, no SiO_2 agglomerations are present in HDPE.

FTIR characterization of interactions in PE*g*MA-SiO_2 masterbatch

The interactions between the surface of SiO_2 nanoparticles and PE*g*MA were investigated by FTIR. FTIR spectra of PE*g*MA (a), SiO_2 (b), and the PEgMA-SiO_2 masterbatch (c) are presented in Figure 5. A new band at 1741 cm^{-1} is seen in the FTIR spectrum of the PE*g*MA-SiO_2 masterbatch, indicating interaction between the maleic anhydride group and a hydroxyl group.[28] Moreover, the intensities of characteristic peaks of the anhydride group of PE*g*MA (C=O stretching) at 1867 and 1792 cm^{-1} are decreased in the spectrum of the PE*g*MA-SiO_2 masterbatch confirming that the anhydride group has reacted. The interaction between the maleic anhydride and hydroxyl groups can be either ester and/or hydrogen bonding.[28,29] The maleic anhydride of PE*g*MA could be interacting with the hydroxyl groups of SiO_2 and/or the hydroxyl group of the stabilizing ethanol left in the mixture to prevent agglomeration of the SiO_2 particles during the solvent exchange procedure. On the other hand, the hydroxyl band of SiO_2 at 3300–3400 cm^{-1} is still present in the IR spectrum of the PE*g*MA-SiO_2 masterbatch, indicating that only part of the hydroxyl groups on the SiO_2 surface have reacted with PE*g*MA.[29]

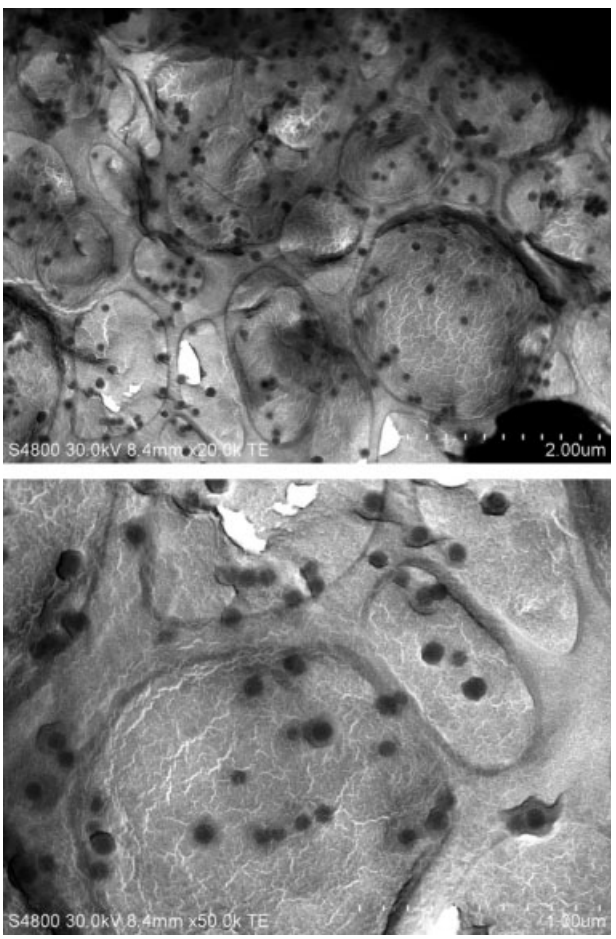

Figure 4 STEM images of dissolved HDPE-PE*g*MA (23 wt %)-SiO_2 (5 wt %) composite obtained from refluxing xylene.

Thermal and mechanical properties of SiO_2 composites

Thermal properties of HDPE, PE*g*MA, the PE*g*MA-SiO_2 masterbatch, and HDPE-PE*g*MA-SiO_2 composites are presented in Table I. According to TGA, the decomposition temperatures (471–473°C) of HDPE nanocomposites were almost independent of SiO_2 content and close to the decomposition temperature of HDPE (467°C). According to DSC measurements, the addition of SiO_2 particles did not change the crystallinities of the HDPE (47.5–50.5%) or PE*g*MA (60.8–59.3%). The crystallization temperatures of HDPE, PE*g*MA, and HDPE-PE*g*MA-SiO_2 composites were all within the range 116–118°C.

Mechanical properties of HDPE-PE*g*MA-SiO_2 composites were measured and compared with those of the reference samples (HDPE and HDPE-PE*g*MA). The results are presented in Table II. Addition of SiO_2 particles and PE*g*MA to HDPE caused a slight increase in Young's modulus, breaking strength, tensile strength, and elongation at break, indicating enhanced toughness of the nanocomposites.

The measured Young's moduli of HDPE-PE*g*MA-SiO_2 nanocomposites were compared with Young's moduli of composites predicted by Mori-Tanaka composite theory. Although the Mori-Tanaka model was developed for composites containing micron-sized fillers, it is also suitable for predicting the properties of nanocomposites since only the shape and volume fraction of the filler are required for modeling of the elastic modulus. As a continuum

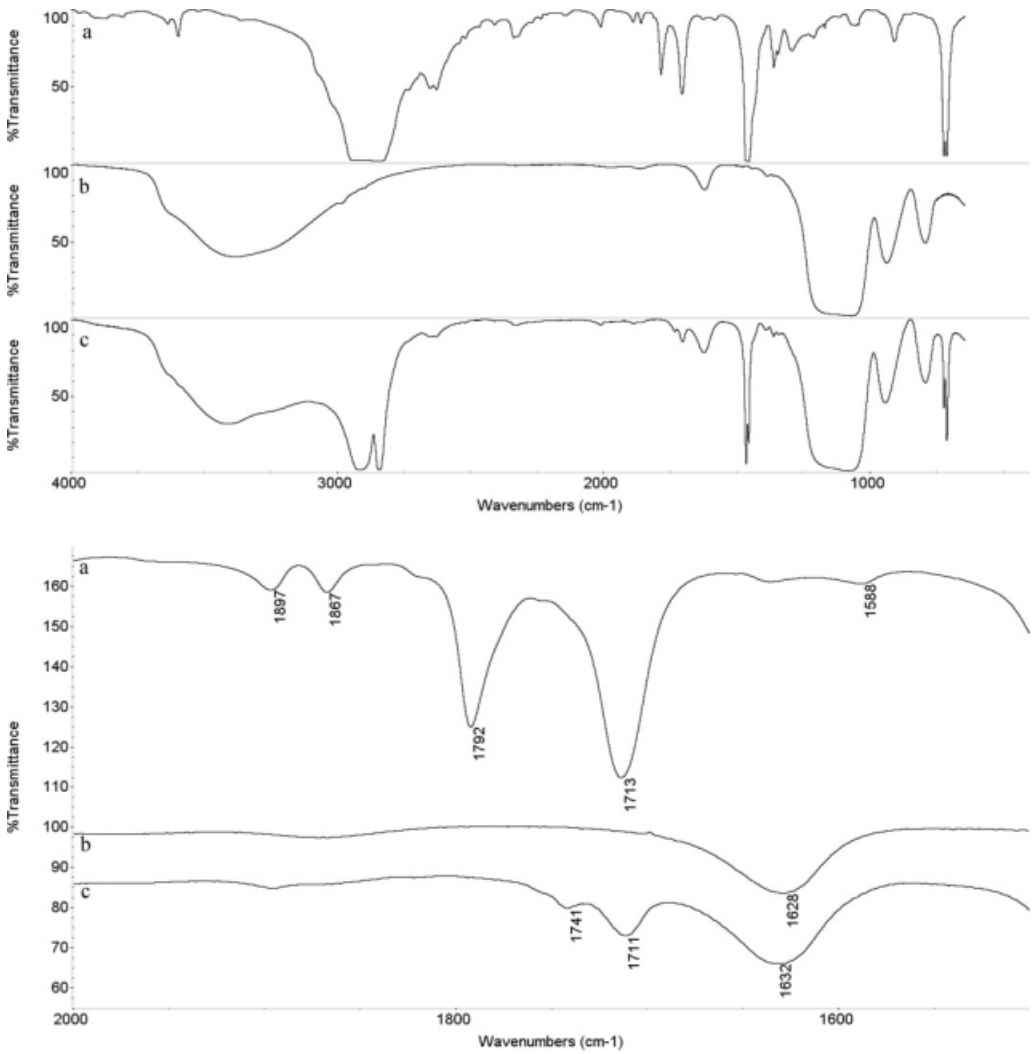

Figure 5 FTIR spectra of PE*g*MA (a), SiO_2 (b), and PE*g*MA-SiO_2 (17.8 wt %) masterbatch (c) with scanning ranges of 600–4000 cm^{-1} and 1500–2000 cm^{-1}.

TABLE I
Thermal Properties of HDPE and HDPE-PEgMA-SiO_2 Composites

Sample (wt % in composite)	Residue at 600°C (wt %)	SiO_2 content (wt %)	Decomposition temperature (°C)	Crystallinity (%)	Crystallization temperature (°C)
HDPE	0.5	–	467 ± 3	47.5 ± 0.3	117.4 ± 0.2
PE*g*MA	0.8	–	468 ± 2	60.8 ± 0.1	116.1 ± 0.7
PE*g*MA-SiO_2 masterbatch		17.8	471 ± 3	59.3 ± 0.5	115.8 ± 0.6
HDPE-PE*g*MA(30)	0.3	–	473 ± 0	49.8 ± 0.4	117.2 ± 0.2
HDPE-PE*g*MA(14)- SiO_2(3)		3.0	472 ± 2	50.5 ± 0.4	118.1 ± 0.1
HDPE- PE*g*MA(23)- SiO_2(5)		5.1	471 ± 2	50.3 ± 0.5	117.8 ± 0.1

TABLE II
Mechanical Properties of HDPE and HDPE-PE*g*MA-SiO_2 Composites

Sample (wt % in composite)	Young's modulus (GPa)	Breaking strength (MPa)	Tensile strength (MPa)	Elongation at break (%)
HDPE	0.57 ± 0.03	12.4 ± 0.7	13.7 ± 0.4	319 ± 49
HDPE-PE*g*MA(15)	0.67 ± 0.06	13.9 ± 1.0	14.8 ± 0.8	395 ± 25
HDPE-PE*g*MA(30)	0.65 ± 0.05	14.3 ± 1.0	15.4 ± 0.8	426 ± 46
HDPE-PE*g*MA(14)- SiO_2(3)	0.66 ± 0.03	14.2 ± 1.0	15.2 ± 0.8	408 ± 33
HDPE- PE*g*MA(23)- SiO_2(5)	0.71 ± 0.05	14.6 ± 0.4	15.5 ± 0.3	443 ± 13

TABLE III
Measured and Predicted Young's Moduli of HDPE-PE*g*MA-SiO_2 Composites

Sample (wt % in composite)	Young's modulus (GPa)	
	Experimental	Mori-Tanaka theory
HDPE	0.57 ± 0.03	
HDPE-PE*g*MA(15)	0.67 ± 0.06	
HDPE-PE*g*MA(30)	0.65 ± 0.05	
HDPE-PE*g*MA(14)-SiO_2(3)	0.66 ± 0.03	0.69
HDPE-PE*g*MA(23)-SiO_2(5)	0.71 ± 0.05	0.68

model, it also assumes that the filler is firmly bonded to the matrix, while the matrix–filler interface is not considered.[20,22] A comparison of the measured and predicted Young's moduli of the HDPE-PE*g*MA-SiO_2 nanocomposites is presented in Table III. The good agreement between the measured and predicted values indicates that there is interaction between the SiO_2 nanoparticles and PE*g*MA, and that the SiO_2 nanoparticles have a reinforcing effect on HDPE-PE*g*MA.

CONCLUSION

Solution mixing starting from a synthesis solution of nanoparticles is a promising method to prepare nanodispersions of SiO_2 in HDPE. Since no drying of nanoparticles is required, the formation of agglomerates is avoided. According to SEM observations, the SiO_2 nanoparticles remain well separated during the solvent exchange and preparation of the masterbatch. The SiO_2 particles are also well dispersed in the final HDPE composites. We conclude that the developed stepwise method provides a useful approach to achieving excellent dispersion of nanoparticles in polyolefins. Given the high level of dispersion of the nanoparticles in HDPE, the improvement in mechanical properties was less than expected, indicating only moderate chemical coupling between SiO_2 nanoparticles and PE*g*MA. Our measured mechanical properties indicate that, besides good dispersion, a stronger interaction of the SiO_2 particles with the HDPE matrix is required for effective tailoring of the properties of composites. The next challenge will be to create stronger interactions between particles and matrix.

References

1. Vaia, R. A.; Maguire, J. F. Chem Mater 2007, 19, 2736.
2. Yuan, Q.; Misra, R. D. K. Mater Sci Tech 2006, 22, 742.
3. Ajayan, P. M.; Schadler, L. S.; Braun, P. V. Nanocomposite Science and Technology; Wiley-VCH: Weinheim, 2003, p 77–153.
4. Rong, M. Z.; Zhang, M. Q.; Ruan, W. H. Mater Sci Tech 2006, 22, 787.
5. Zhang, M. Q.; Rong, M. Z.; Friedrich, K. Encyclopedia of Nanoscience and Nanotechnology; Nalwa, H. S., Ed. American Scientific Publishers: California, 2004; Vol. 7, 125–160.
6. Stöber, W.; Fink, A.; Bohn, E. J Colloid Interf Sci 1968, 26, 62.
7. Green, D. L.; Jayasundara, S.; Lam, Y.-F.; Harris, M. T. J Non--Cryst Solids 2003, 315, 166.
8. Jia, Q. M.; Zheng, M.; Xu, C. Z.; Chen, H. X. Polym Adv Technol 2006, 17, 168.
9. Wu, T.; Ke, Y. Eur Polym J 2006, 42, 274.
10. Costa, C. A. R.; Valadares, L. F.; Galembeck, F. Colloid Surf A 2007, 302, 371.
11. Giraldo, L. F.; Echeverri, M.; López, B. L. Macromol Symp 2007, 258, 119.
12. Riello, P.; Munarin, M.; Silvestrini, S.; Moretti, E.; Storaro, L. J Appl Cryst 2008, 41, 985.
13. Tang, W.; Santare, M. H.; Advani, S. G. Carbon 2003, 41, 2779.
14. Hua, Y.-Q.; Zhang, Y.-Q.; Wu, L.-B.; Huang, Y.-Q.; Wang, G.-Q. J Macromol Sci B 2005, 44, 149.
15. Wang, W.-Y.; Zeng, X.-F.; Wang, G.-Q.; Chen, J.-F. J Appl Polym Sci 2007, 106, 1932.
16. Chaichana, E.; Jongsomjit, B.; Praserthdam, P. Chem Eng Sci 2007, 62, 899.
17. Rong, J.; Jing, Z.; Li, H.; Sheng, M. Macromol Rapid Commun 2001, 22, 329.
18. Liang, G.; Xu, J.; Bao, S.; Xu, W. J Appl Polym Sci 2004, 91, 3974.
19. Mori, T.; Tanaka, K. Acta Metall 1973, 21, 571.
20. Fornes, T. D.; Paul, D. R. Polymer 2003, 44, 4993.
21. Tandon, G. P.; Weng, G. J. Polym Compos 1984, 5, 327.
22. Odegard, G. M.; Clancy, T. C.; Gates, T. S. Polymer 2005, 46, 553.
23. Hirao, K.; Tanaka, K.; Furukawa, S.; Soga, N. J Mater Sci Lett 1995, 14, 697.
24. Jo, C.; Naguib, H. E. Polymer 2007, 48, 3349.
25. Bliznakov, E. D.; White, C. C.; Shaw, M. T. J Appl Polym Sci 2000, 77, 3220.
26. Tolnai, G.; Csempesz, F.; Kabai-Faix, M.; Kálmán, E.; Keresztes, Z.; Kovács, A. L.; Ramsden, J. J.; Hórvölgyi, Z. Langmuir 2001, 17, 2683.
27. Ghosh, S. K.; Deguchi, S.; Mukai, S.; Tsujii, K. J Phys Chem B 2007, 111, 8169.
28. Paunikallio, T.; Kasanen, J.; Suvanto, M.; Pakkanen, T. T. J Appl Polym Sci 2003, 87, 1895.
29. Bikiaris, D. N.; Vassiliou, A.; Pavlidou, E.; Karayannidis, G. P. Eur Polym J 2005, 41, 1965.